Intervertebral Disc Segmentation and Volumetric Reconstruction From Peripheral Quantitative Computed Tomography Imaging

Alexander Wong*, Akshaya Mishra, Justin Yates, Paul Fieguth, David A. Clausi, and Jack P. Callaghan

Abstract—An automatic system for segmenting and constructing volumetric representations of excised intervertebral discs from peripheral quantitative computed tomography (PQCT) imagery is presented. The system is designed to allow for automatic quantitative analysis of progressive herniation damage to the intervertebral discs under flexion/extension motions combined with a compressive load. Automatic segmentation and volumetric reconstruction of intervertebral disc from PQCT imagery is a very challenging problem due to factors such as streak artifacts and unclear material density separation between contrasted intervertebral disc and surrounding bone in the PQCT imagery, as well as the formation of multiple contrasted regions under axial scans. To address these factors, a novel multiscale level set approach based on the Mumford–Shah energy functional in iterative bilateral scale space is employed to segment the intervertebral disc regions from the PQCT imagery. A Delaunay triangulation is then performed based on the set of points associated with the intervertebral disc regions to construct the volumetric representation of the intervertebral disc. Experimental results show that the proposed system achieves segmentation and volumetric reconstructions of intervertebral discs with mean absolute distance error below 0.8 mm when compared to ground truth measurements. The proposed system is currently in operational use as a visualization tool for studying progressive intervertebral disc damage.

Index Terms—Bilateral, computed tomography (CT), intervertebral disc, Mumford–Shah, scale space, segmentation, volumetric reconstruction.

I. INTRODUCTION

ONE of the most common musculoskeletal disorders faced in industrialized countries is low back pain [1]. While the factors that contribute to low back pain can vary, a frequent source of low back pain is damage to the intervertebral discs, which act as shock absorbers between the individual vertebrae.
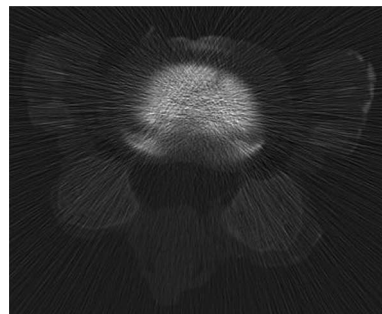
Fig. 1. Axial CT image slice of the excised intervertebral disc and surrounding vertebral regions. The intervertebral disc is represented by the bright regions due to the injected contrast agent.

In particular, studies have shown that the major factors contributing to intervertebral disc damage are flexion/compressive motions [2] and compressive load [3]. Hence, to improve the understanding of intervertebral disc damage, it is necessary to study and quantify the migration of herniated intervertebral discs under flexion/extension motions combined with a compressive load.

In established nondestructive approaches, progressive intervertebral disc herniation damage was studied using standard X-ray radiographic imagery. However, comparative studies have demonstrated that such approaches show discordance with destructive "gold standard" dissection techniques [4], [5]. A promising new nondestructive approach for studying intervertebral disc damage is the use of computed tomography (CT). To study progressive intervertebral disc herniation, a contrast agent is injected into the excised intervertebral disc prior to being imaged using CT. A typical axial CT image slice of the excised intervertebral disc and surrounding vertebral regions is shown in Fig. 1, where the intervertebral disc is represented by the bright regions due to the injected contrast agent. One of the advantages of CT imagery over traditional X-ray radiographic imagery is that CT provides improved resolution and material density sensitivity, and as such holds the potential to better illustrate actual disc damage previously observed using dissection techniques without damaging the specimen. Therefore, a model of herniation damage constructed from CT imagery may allow a better visualization of herniation damage without specimen destruction, and holds the potential to add valuable information regarding herniation progression and specific pathways of damage.

The visualization and quantitative analysis of progressive intervertebral disc herniation damage requires the automatic

segmentation and volumetric reconstruction of intervertebral discs from the acquired CT imagery, which is a very challenging problem for several reasons. First, multiple contrasted regions are formed under axial CT scans, requiring multiple regions to be segmented in the image. Second, the material density separation between the contrasted intervertebral disc regions and the surrounding bone regions is unclear and appears blurred in the CT image, making the isolation of the intervertebral disc difficult. Third, a basic assumption made in CT imaging is that some transmitted radiation is observed by each detector at every position [6]. However, the presence of a high density material can significantly reduce transmission to an extent that a detector observes no transmission. The high density material in the case of studying intervertebral disc herniation using CT imagery is the contrast agent injected into the intervertebral disc. This violation in the basic assumption of CT imaging results in streaking artifacts in the reconstructed image, which is very noticeable in Fig. 1. The proposed method addresses these issues to provide accurate segmentation and volumetric reconstruction.

The main contribution of this paper is an automated system for segmentation and volumetric reconstruction of intervertebral disc from axial peripheral quantitative computed tomography (PQCT) imagery. To the best of the authors' knowledge, there is no research literature associated with automatic segmentation and volumetric reconstruction of intervertebral disc. While there is existing research literature on automatic segmentation of intervertebral discs [7], [8], these approaches deal with sagittal magnetic resonance (MR) imagery, where the boundaries of the intervertebral discs are clear, exhibit few imaging artifacts, and the appearance of the discs from a sagittal perspective is relatively simple and remain a single region. Therefore, these approaches can utilize simple watershed and other edge-based segmentation methods to provide good segmentation accuracy. However, none of these methods are useful for accurate intervertebral disc segmentation from axial PQCT imagery where the disc boundaries are unclear, highly complex, and exhibit strong streaking artifacts. PQCT was chosen for the study of intervertebral disc damage primarily due to its cost and convenience when compared to MR, particularly for excised functional spinal units.

II. MATERIALS AND METHODS

The materials and methods used to study progressive intervertebral disc herniation under flexion/extension motions combined with a compressive load can be described as follows. A solution consisting of 0.4 mL of radioopaque contrast agent (Omnipaque, General Electric Company) and 0.15 mL of blue dye was injected into the intervertebral discs of excised porcine functional spinal units. Damage in the form of intervertebral herniations was created by loading the specimens in a servohydraulic testing system under combined compressive loading with repeated flexion/extension motions [9]. Three sets of CT images were then obtained; prior to loading, after sufficient cycles of load to cause partial damage to the intervertebral disc, and again after additional loading hypothesized to exacerbate herniation damage. The CT images were taken through the level of the intervertebral disc using a Stratec Medizintechnik XCT 2000 Research Plus PQCT scanner. Each of the three sets of CT images consists

of eight serial slices spanning the entire intervertebral disc using a slice thickness of 0.9 mm, a scan speed of 10 mm/s, and implementing a voxel size of 0.2 mm × 0.2 mm × 0.2 mm.

For each set of CT images, the contrasted intervertebral disc regions are then segmented from the surrounding bone structures using a multiscale level set approach based on the Mumford–Shah energy functional in iterative bilateral scale space, which is described in Section II-A. A volumetric reconstruction of intervertebral disc is then constructed from the segmented intervertebral disc regions using Delaunay triangulation [10], which is described in Section II-B.

A. Multiscale Segmentation in Iterative Bilateral Scale Space

The first step in the proposed system is to segment the contrasted intervertebral disc regions from the PQCT imagery. One of the most common methods for image segmentation is based on the minimization of the Mumford–Shah energy functional [11]. Let the image u_0 be a piecewise smooth function that is well approximated by a set of smooth functions u_i defined on a set of regions R_i covering plane domain R. In our case, u_0 is a function of material density and the set of regions R_i is defined as the contrasted invertebral disc and surrounding bone regions. The segmentation problem can then be defined as determining the decomposition $R = R_1 \bigcup \cdots \bigcup R_n$ of u_0 that provides the optimal estimate of u_0 by a set of smooth functions $u_1, \ldots, u_n$. The decomposition of u_0 can be obtained by minimizing the Mumford–Shah energy functional, which indicates the degree of match between u_0 and the estimated decomposition

$$\hat{R} = \arg \min_R \left[\alpha \oint_R (u - u_0)^2 \, d\underline{x} + \oint_{R-\Gamma} \|\nabla u\|^2 \, d\underline{x} + \beta \, |\Gamma| \right] \tag{1}$$

where Γ is the boundary between regions, $|\Gamma|$ is the total arclength of Γ, and α and β control the penalty terms.

The three main issues discussed in Section I associated with multiple regions, unclear density separation between the contrasted regions and surrounding regions, and streaking artifacts must be addressed to provide accurate intervertebral segmentation results using the Mumford–Shah energy minimization approach. An effective approach for addressing the issue associated with multiple contrasted regions is to use the level set method [12] for minimizing the Mumford–Shah energy functional. One of the main advantages of using the level set method is that it automatically handles topological changes, thus making it well suited for segmenting multiple contrasted intervertebral disc regions within the same CT image. To minimize the Mumford–Shah energy functional using the level set method, Γ is treated as a zero level set function ϕ_0 of a surface ϕ and evolved based on a partial differential equation toward the minimum energy potential.

To address the issues associated with streaking artifacts and unclear region separation, we propose a novel multiscale extension to solving the Mumford–Shah energy minimization problem in an iterative bilateral scale space. While linear and nonlinear scale-space extensions to the Mumford–Shah energy minimization problem have been previously proposed [13], such approaches provide poor coarse-scale structure preservation and

localization, which can lead to poor segmentation accuracy. To address these issues, we introduce the concept of iterative bilateral scale space, which is inspired by the bilateral filtering scheme proposed by Tomasi and Manduchi [14], where detail in an image is smoothed based not only on spatial locality but also photometric differences. We take the fundamental concept behind bilateral filtering and extend it based on scale-space theory [15], where a multiscale decomposition of an image is formed such that image detail is monotonically removed at each subsequent scale. The key advantage of iterative bilateral scale space over existing linear and nonlinear scale spaces is that coarse-scale structures are well preserved and localized, while fine-scale structures such as streaking artifacts and other artifacts that affect region boundary clarity are suppressed.

For a given image u_0, the iterative bilateral scale-space representation is defined by a family of derived images L_t

$$L_t(\underline{x}) = \frac{\sum_{\psi} w_p(\underline{x}, \psi) w_s(\underline{x}, \psi) L_{t-1}(\underline{x})}{\sum_{\psi} w_p(\underline{x}, \psi) w_s(\underline{x}, \psi)} \qquad (2)$$

where $L_0 = u_0$, t is the scaling parameter, ψ defines a local neighborhood, and w_p and w_s denote Gaussian photometric and spatial weights on $\underline{x}$, respectively

$$w_p(\underline{x}, \psi) = \exp\left[-\frac{1}{2}\left(\frac{\|L_{t-1}(\underline{x}) - L_{t-1}(\psi)\|}{\sigma_p}\right)^2\right] \qquad (3)$$

$$w_s(\underline{x}, \psi) = \exp\left[-\frac{1}{2}\left(\frac{\|\underline{x} - \psi\|}{\sigma_s}\right)^2\right]. \qquad (4)$$

By solving the Mumford–Shah energy minimization problem across multiple scales in iterative bilateral scale space, we are able to evolve Γ to converge around the contrast intervertebral disc regions while avoiding local minima caused by streaking artifacts and other fine scale artifacts. Based on the previous iterative bilateral scale-space formulation, the proposed multiscale segmentation method can be described as follows. Let L be the iterative bilateral scale-space representation of u_o at k scales. At scale $t - 1$, an estimate of R is determined by minimizing the Mumford–Shah energy functional for L_{t-1} using the functions $u_{1,t}, \ldots, u_{n,t}$ associated with the estimate of R at t as the initial condition

$$\hat{R}_{t-1} = \underset{R_{t-1}}{\arg\min}\left[\alpha \oint_R (u - L_{t-1})^2\, d\underline{x}\right.$$
$$\left. + \oint_{R-\Gamma} \|\nabla u\|^2\, d\underline{x} + \beta\, |\Gamma| \right]. \qquad (5)$$

This hierarchical estimation process is performed going from the coarsest scale to the finest scale to obtain the final segmented regions $\hat{R} = \hat{R}_0$. Based on testing, setting the number of scales to three ($t = \{0, 1, 2\}$) was found to be effective and is used for all tests. The intervertebral disc regions are then determined automatically from the resulting contours based on the intensity distributions of the contrast agent. This is accomplished by comparing the learned histogram of the contrast agent with that of the resulting contours, and the contours with intensities that are likely to belong to the distribution of the contrast agent are selected.

TABLE I
MAD ERROR, STANDARD DEVIATION, AND p-VALUE FROM PAIRED t-TEST BETWEEN PROPOSED METHOD, AND TMS AND LSSMS

Method	MAD (mm) (p-value)		
	Test 1	Test 2	Test 3
TMS	1.30±0.96 (**0.0015**)	1.68±1.20 (**0.0015**)	2.60±1.60 (**0.0001**)
LSSMS [13]	0.85±0.67 (**0.0267**)	0.95±0.80 (**0.1117**)	1.57±0.85 (**0.0014**)
Proposed	0.45±0.15 (**1.0000**)	0.60±0.30 (**1.0000**)	0.76±0.35 (**1.0000**)

Each test set contains two disc samples.

B. Volumetric Reconstruction

Based on the segmented contrasted intervertebral disc regions obtained during the segmentation process, a set of q points $P = \{\underline{p}_1, \ldots, \underline{p}_q\}$ is extracted along the intervertebral disc boundaries to represent points along the surface of the intervertebral disc. A Delaunay triangulation [10] $D(P)$ is then performed based on P to construct the volumetric representation of the intervertebral disc. The Delaunay triangulation, in the case of 3-D spaces, is based on the criteria that the circumscribed spheres of all triangles in $D(P)$ must not contain points other than the three points defining the triangle itself. The problem of computing the Delaunay triangulation of P is solved using the Quickhull algorithm [16].

III. EXPERIMENTAL RESULTS

To evaluate the effectiveness of the proposed system, segmentation and volumetric reconstruction were performed on three test sets of serial PQCT images acquired from the porcine functional spinal units at three different times.

Test 1: Prior to applying flexion/extension motions with compressive load.
Test 2: After 7000 cycles of flexion/extension motions with a 1.5 kN compressive load to cause partial damage to the intervertebral disc [9].
Test 3: After additional cycles of vibrational motions to exacerbate herniation.

Each test set consists of 16 slices consisting of two different entire intervertebral disc samples and are representative of nonideal, real-world scenarios, where the PQCT images are characterized by streaking artifacts and unclear separation between contrasted intervertebral disc and surrounding bone regions. The proposed system was implemented in MATLAB and tested on an Intel Pentium 4, 3-GHz machine with 1 GB of RAM. Each intervertebral disc took approximately 2 min to reconstruct. For comparison purposes, the traditional Mumford–Shah (TMS) and linear scale-space extension to Mumford–Shah [13] (LSSMS) were also tested.

The mean absolute distance (MAD) error between the ground truth measurements by a trained expert and the obtained intervertebral disc regions using the proposed system, along with the standard deviation, is computed over all images within the test sets. Given an interobserver variability of approximately 1 mm, which was determined based on the MAD error between the 48 manual segmentations by two in-house experts, a MAD error below 1 mm is typically considered useful accuracy. The MAD error results for all three test sets are shown in Table I.
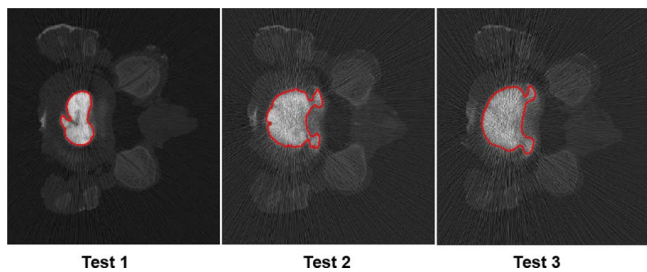
Fig. 2. Sample intervertebral disc segmentation results from first disc sample. Visually, the proposed system was able to segment the contrasted intervertebral disc regions with a high level of accuracy for all tests.
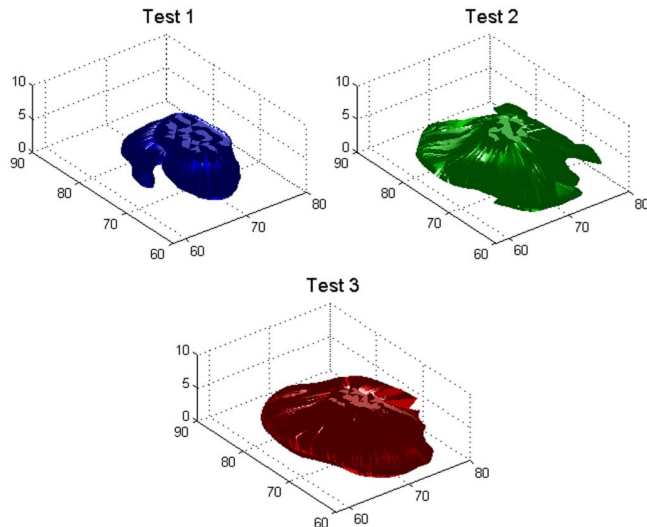

Fig. 3. Volumetric representations of first intervertebral disc sample.

The reduction in MAD error using the proposed system over the other two tested methods was found to be statistically significant based on paired t-tests, with all tests having MAD error below 0.8 mm. The MAD error increases as the amount of herniation damage increases, which can be attributed to the fact that the shape of the intervertebral disc becomes increasingly distorted, and thus becomes more difficult to segment accurately. Sample segmentation results from the first disc sample are shown in Fig. 2. Visually, the proposed system was able to segment the contrasted intervertebral disc regions with a high level of accuracy for all tests. This demonstrates the effectiveness of the proposed method in segmenting intervertebral disc regions from PQCT imagery. The volumetric representations of the first intervertebral disc sample are shown in Fig. 3. Such representations show very clearly the change in intervertebral disc shape from normal conditions (test 1) to herniation conditions (tests 2 and 3) and provides a clear indication of mechanical damage to the tissues of the annulus fibrosus that has allowed the nucleus pulposus to progress in the disc herniation process. The proposed system is currently in operational use as a visualization tool to study progressive intervertebral disc damage.

IV. CONCLUSION AND FUTURE WORK

In this paper, we have introduced an automatic approach to the problem of intervertebral disc segmentation and volumetric reconstruction from PQCT imagery. A novel multiscale level set scheme based on a Mumford–Shah model in bilateral scale space was introduced for segmenting contrasted intervertebral disc regions from the serial PQCT images. A Delaunay triangulation approach was employed for constructing a volumetric representation of the intervertebral disc based on the segmented contrasted regions. Experimental results showed that accurate segmentations of intervertebral disc can be achieved from PQCT image sequences. The system is currently in operational use for visualizing and studying intervertebral disc damage. Future work involves extracting detailed volume and shape information from the extracted 3-D volumes.

REFERENCES

[1] N. Hadler, "Work disability and musculoskeletal disease," *Arthritis Rheum.*, vol. 29, pp. 1410–1411, 1986.

[2] W. Marras, S. Lavender, S. Leurgans, S. Rajulu, W. Allread, F. Fathallah, and S. Ferguson, "The role of dynamic three-dimensional trunk motion in occupationally-related low back disorders. The effects of workplace factors, trunk position, and trunk motion characteristics on risk of injury," *Spine*, vol. 18, pp. 617–628, 1993.

[3] R. Norman, R. Wells, P. Neumann, J. Frank, H. Shannon, and M. Kerr, "A comparison of peak vs. cumulative physical work exposure risk factors for the reporting of low back pain in the automotive industry," *Clin. Biomech.*, vol. 13, pp. 561–573, 1998.

[4] C. Tampier, J. Drake, J. Callaghan, and S. McGill, "Progressive disc herniation: An investigation of the mechanism using radiologic, histochemical, and microscopic dissection techniques on a porcine model," *Spine*, vol. 32, pp. 2869–2874, 2007.

[5] S. Gordon, K. Yang, P. Mayer, A. Mace, V. Kish, and E. Radin, "Mechanism of disc rupture: A preliminary report," *Spine*, vol. 164, pp. 450–456, 1991.

[6] T. Curry, J. Dowdey, and R. Murry, *Christensen's Physics of Diagnostic Radiology*, 4th ed. Philadelphia, PA: Lippincott/Williams & Wilkins, 1990.

[7] C. Chevrefils, F. Cheriet, G. Grimard, and C. Aubini, "Watershed segmentation of intervertebral disk and spinal canal from MRI images," in *Proc. ICIAR*, 2007, pp. 1017–1027.

[8] S. Seifert, I. Wachter, and R. Dillmann, "Segmentation of intervertebral discs, trachea and spinal cord from MRI images," in *Proc. Comput. Assist. Radiol. Surg.*, Osaka, Japan, 2006.

[9] J. Callaghan and S. McGill, "Intervertebral disc herniation: Studies on a porcine model exposed to highly repetitive flexion/extension motion with compressive force," *Clin. Biomech.*, vol. 16, pp. 28–37, 2001.

[10] L. Guibas, D. Knuth, and M. Sharir, "Randomized incremental construction of Delaunay and Voronoi diagrams," *Algorithmica*, vol. 7, pp. 381–413, 1992.

[11] D. Mumford and J. Shah, "Optimal approximation by piecewise smooth functions and associated variational problems," *Commun. Pure Appl. Math.*, vol. 42, pp. 577–685, 1989.

[12] S. Osher and J. Sethian, "Fronts propagating with curvature dependent speed: Algorithms based on Hamilton–Jacobi formulations," *J. Comput. Phys.*, vol. 79, pp. 12–49, 1988.

[13] C. Alvino and A. Yezzi, "Fast Mumford–Shah segmentation using image scale space bases," *Proc. SPIE*, vol. 6498, pp. 64980F-1–64980F-10, 2007.

[14] C. Tomasi and R. Manduchi, "Bilateral filtering for gray and color images," in *Proc. IEEE Int. Conf. Comput. Vis.*, Bombay, India, 1998, pp. 839–846.

[15] T. Lindeberg, "Scale-space theory: A basic tool for analysing structures at different scales," *J. Appl. Stat.*, vol. 21, no. 2, pp. 224–270, 1994.

[16] C. Barber, D. Dobkin, and H. Huhdanpaa, "The Quickhull algorithm for convex hulls," *ACM Trans. Math. Softw.*, vol. 22, no. 4, pp. 469–483, 1996.